

Figure S1. Thermogravimetric analysis of powdered milk.

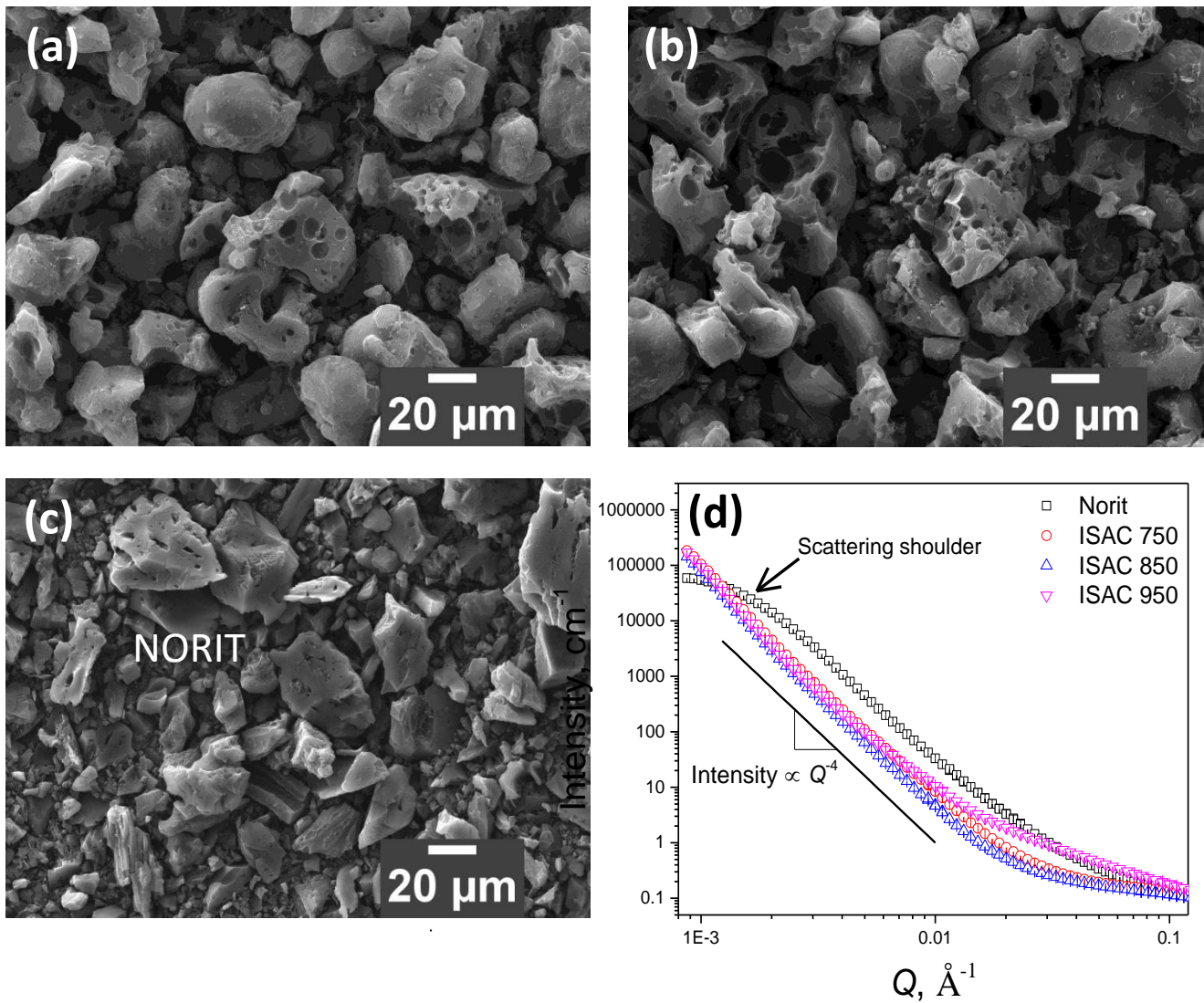


Figure S2. SEM micrographs (a) ISAC 750, (b) ISAC 950, (c) baseline Norit, (d) SANS curves of ISAC 750, ISAC 850, ISAC 950 and Norit.

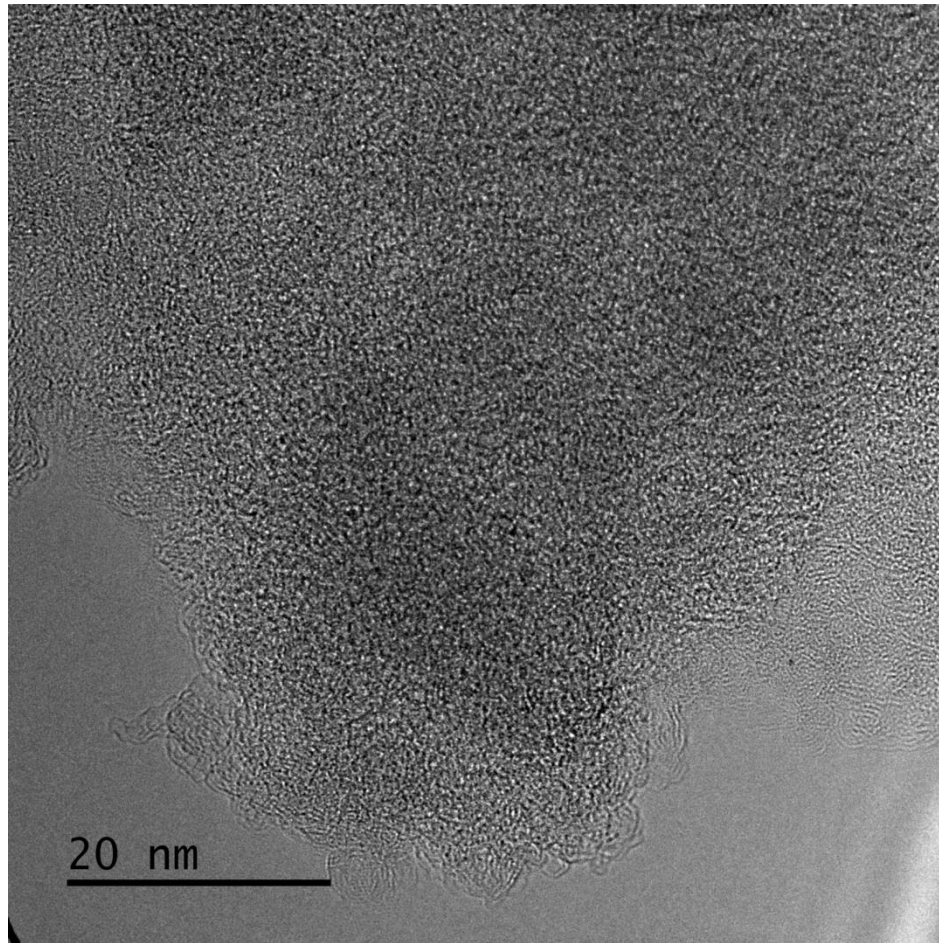


Figure S3. HRSEM micrographs of baseline Norit.

### Surface Composition (at.%)

	C	O	N	Cl	Al	S	K	P	Na
Milk	65.2	29.3	4.2	.3	0	0.2	0.3	0.3	0.2

### Surface Composition (at.%)

	C	O	Si	Cl	N	Na
ISAC-750	93.6	3.6	2.2	0.1	0.5	0.0
ISAC-850	97.2	2.3	0.1	0.1	0.3	0.0
ISAC-950	95.9	3.0	0.3	0.5	0.3	0.0
Norit-Supra	96.2	3.3	0.2	0.0	0.0	0.3

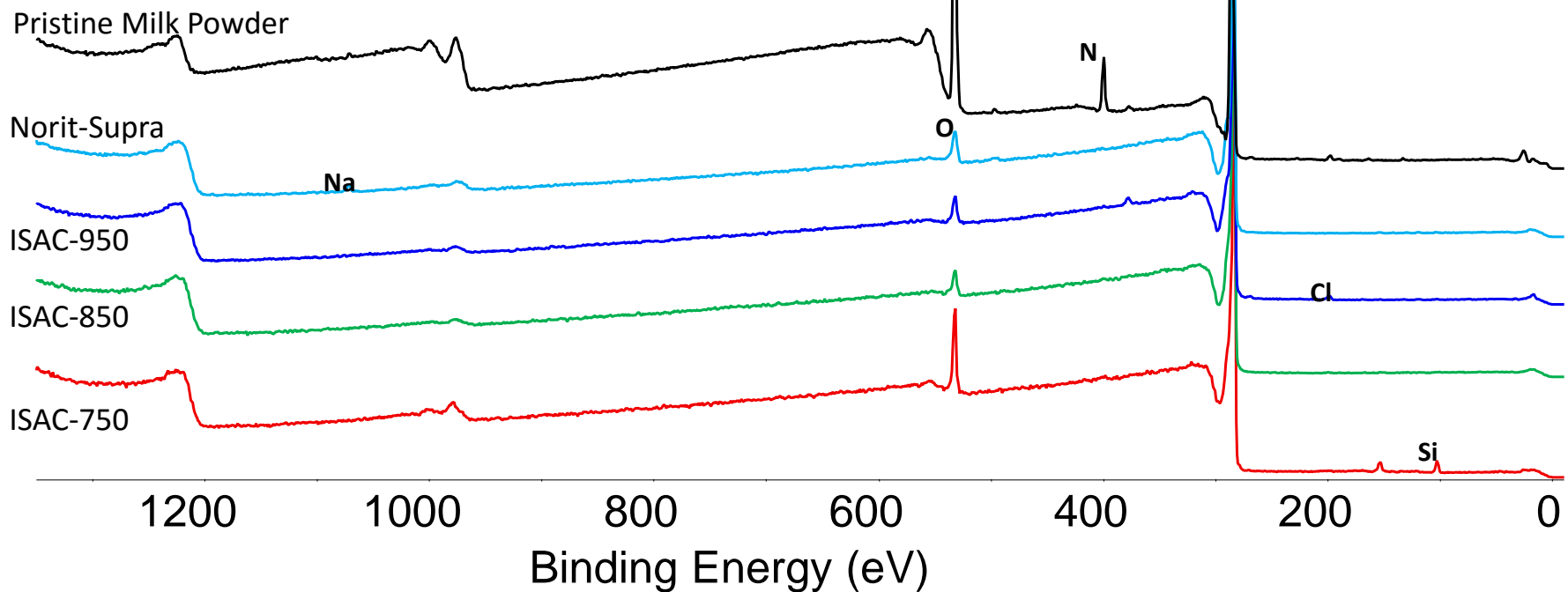
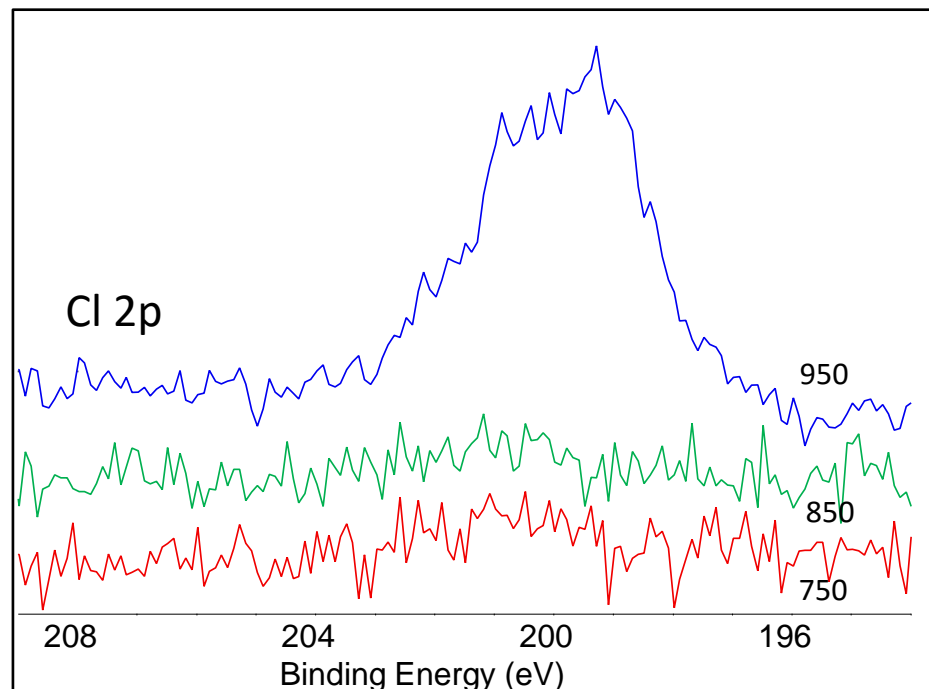
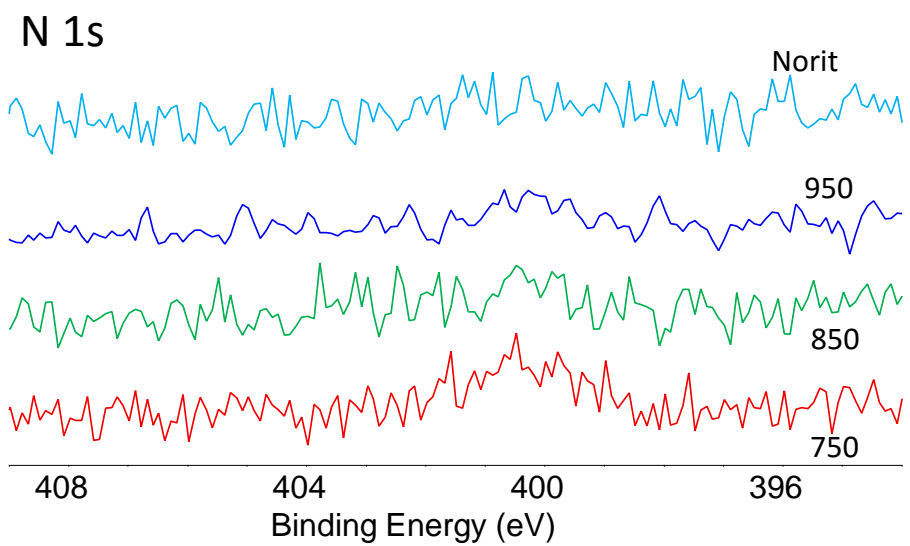
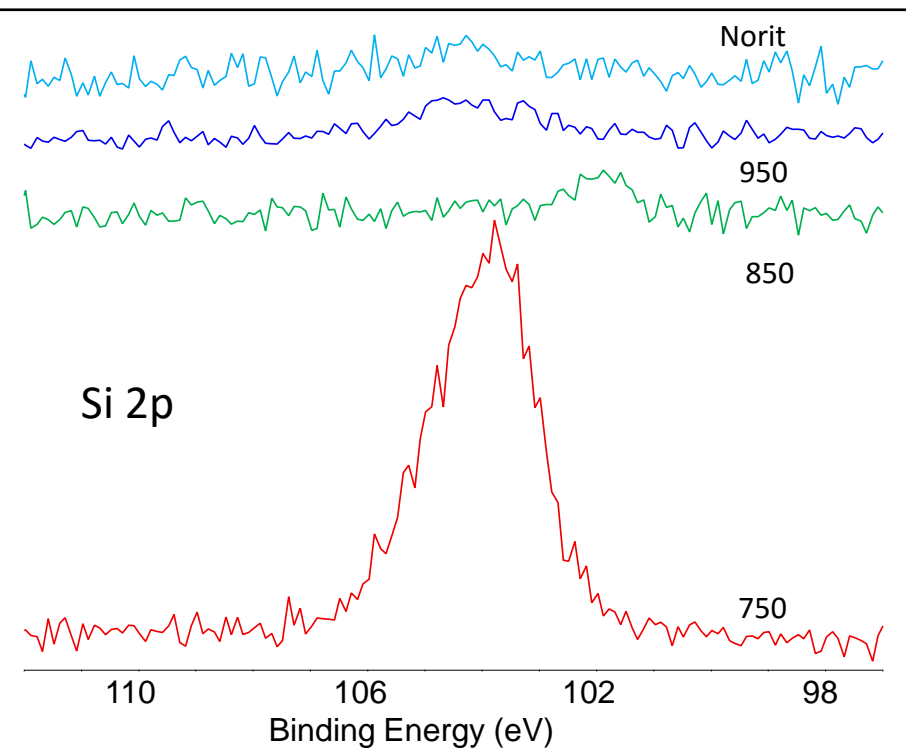
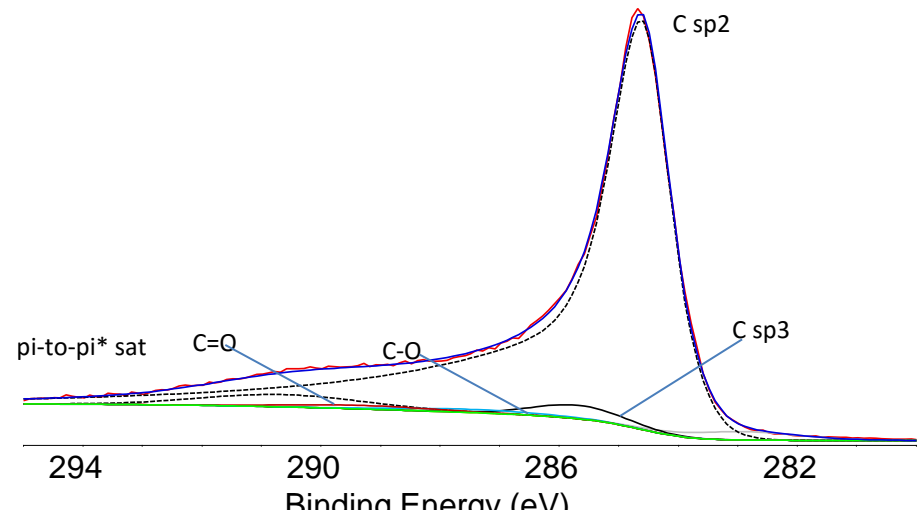


Figure S4. X-ray Photoelectron Spectroscopy (XPS) analysis. The four samples (ISAC-750, -850, -950, and Norit) were examined at the same time. The powders were dispersed on double-sided tape and data were collected using the charge compensation flood gun. The sp2 carbon was set to 284.6 eV for all samples. Milk Powder was analyzed separately.

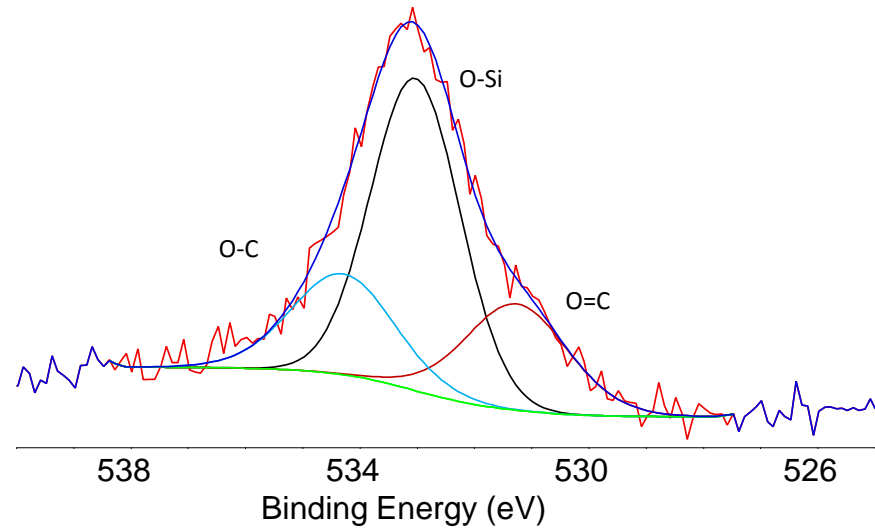
Comparison of the Si 2p, N 1s, and Cl 2p spectra for the samples.



ISAC-750

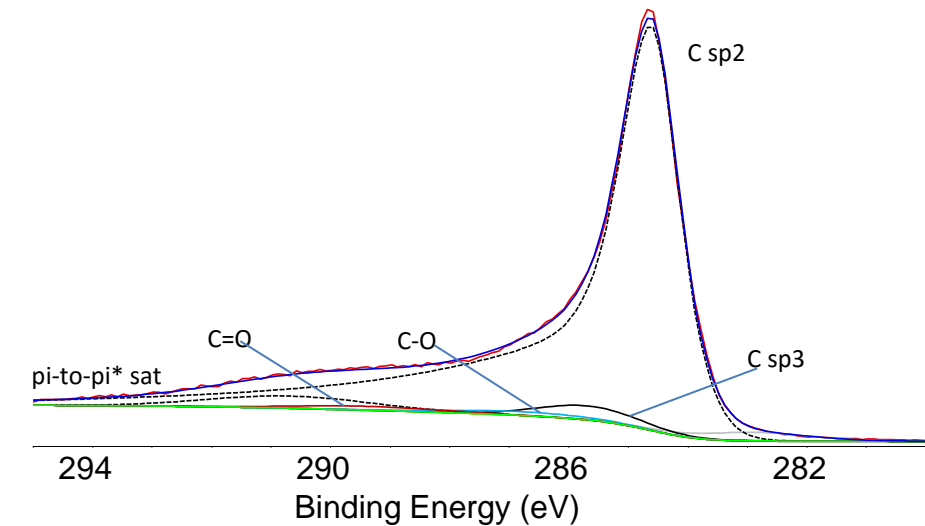


C 1s

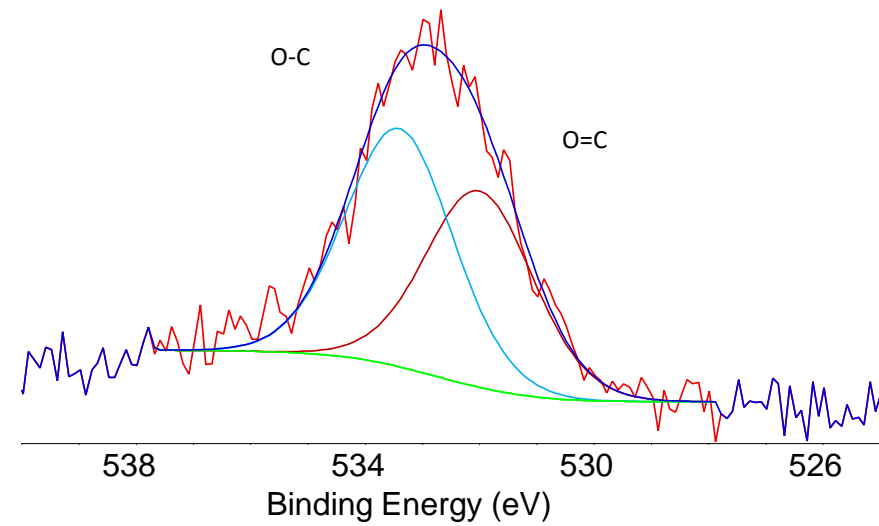


O 1s

ISAC-850

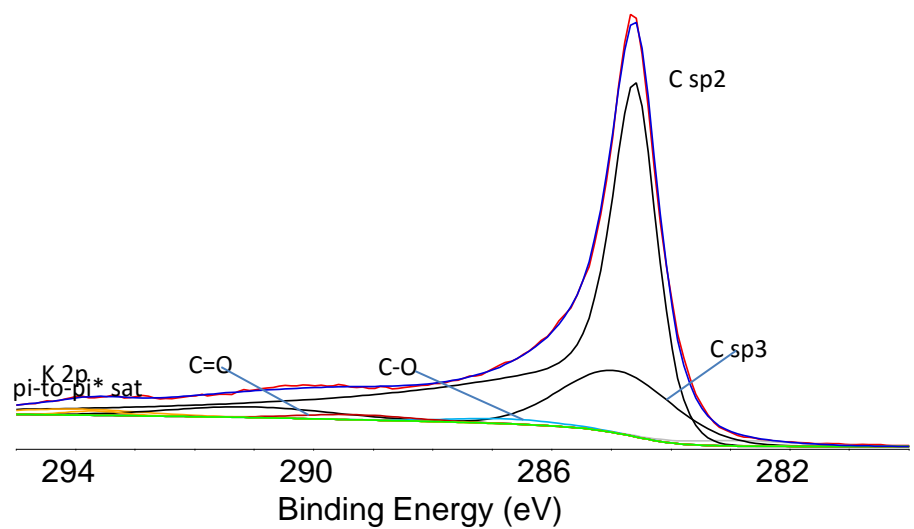


C 1s

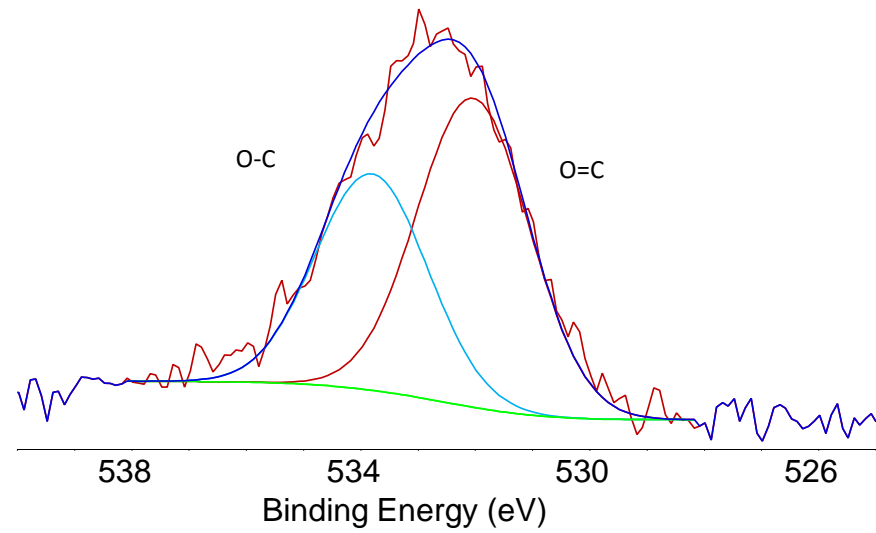


O 1s

ISAC-950

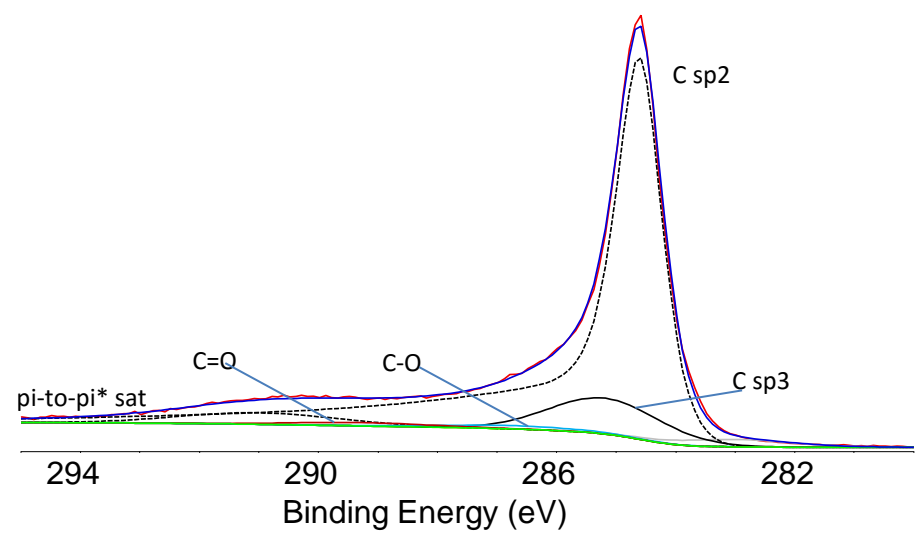


C 1s

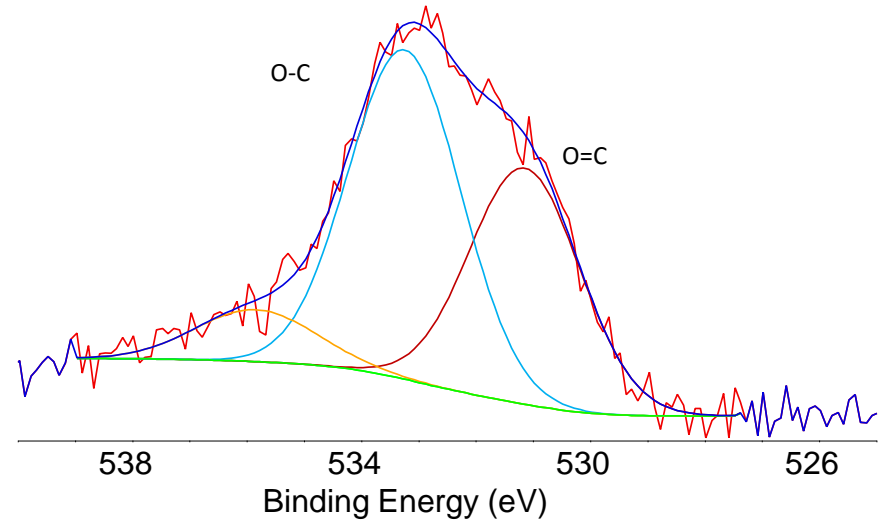


O 1s

# Norit



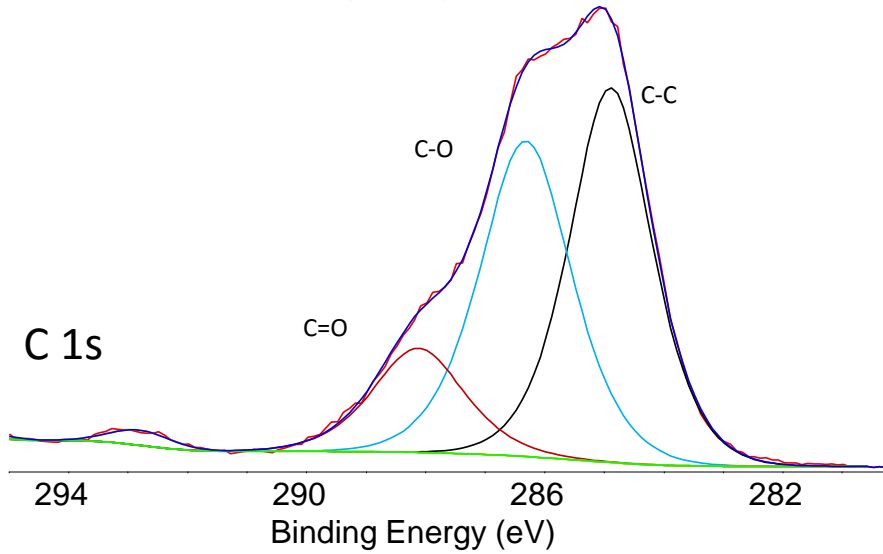
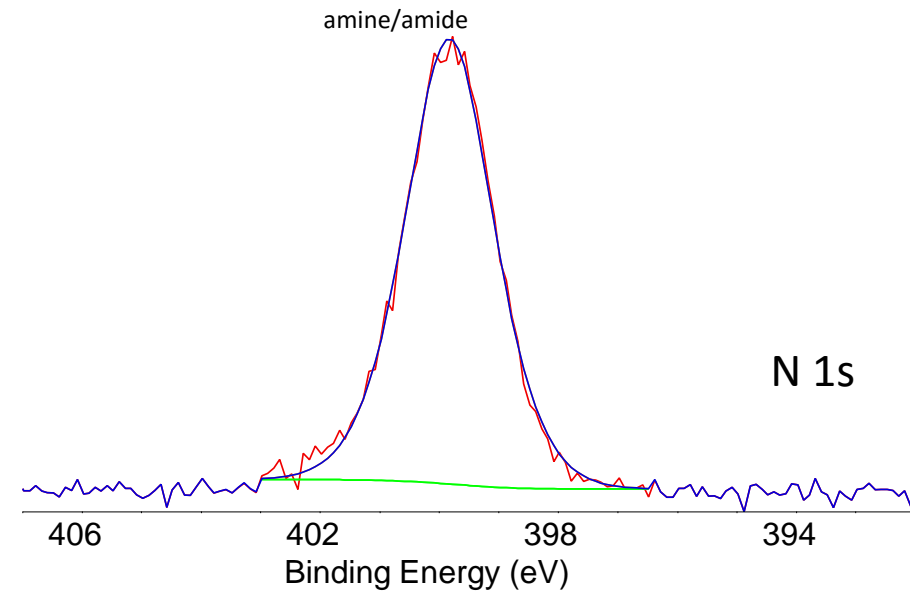
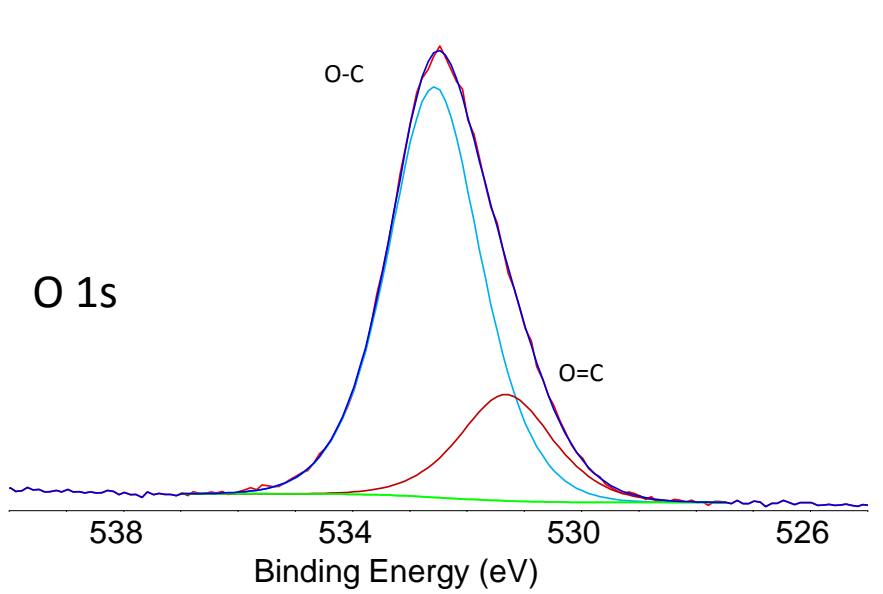
C 1s



O 1s

## Milk Powder

The O 1s, N 1s, and C 1s core level spectra are shown. The O 1s shows two components assigned to O-C bonding (blue) and O=C bonding (red). The C 1s was fit with three components, C-C, C-O, and C=O. and the amounts correlate with the O 1s features. Some of the C 1s bonding is associated with C/N bonds, but is simply folded into the C-O and C=O features. N 1s shows a single feature due to amine or amide type bonding.



Name	At. %
C (C-C)	29.1
C (C-O)	27.1
C (C=O)	9.0
O (O-C)	23.3
O (O-C)	6.0
N (amine/amide)	4.2
S	0.2
K	0.3
P	0.3
Cl	0.3
Na	0.2

isac-750		isac-850		isac-950		Norit		Milk Powder		
B.E	at.%	B.E	at.%	B.E	at.%	B.E	at.%	Name	At. %	
C (sp2)	284.6	89.2	284.6	91.9	76.7	284.6	83.2	C (C-C)	29.1	
C (sp3)	285.7	2.5	285.7	3.0	284.9	16.6	285.2	10.5	C (C-O)	27.1
C (C-O)	287.4	0.9	286.8	1.2	286.8	1.3	286.7	1.2	C (C=O)	9.0
C (C=O)	289.4	1.0	289.4	1.2	289.3	1.3	289.3	1.3	O (O-C)	23.3
O (O-C)	534.3	0.8	533.4	1.3	533.8	1.2	533.2	1.9	O (O-C)	6.0
O (O=C)	531.3	0.8	532.0	1.1	532.0	1.8	531.2	1.4	N (amine/amide)	4.2
O (O-Si)	533.0	2.0		0.0		0.0		S	0.2	
Na	400.6	0.5	403.8	0.3	400.8	0.3	0.0	K	0.3	
Si	103.9	2.2	101.8	0.1	104.7	0.3	106.0	P	0.3	
Cl	200.5	0.1	201.2	0.1	199.6	0.5	0.0	Cl	0.3	
Na	0.0		0.0		0.0		1072.0	0.3	Na	0.2

Table S1. A table summarizing the results of the C 1s and O 1s peak fits of the XPS spectra.

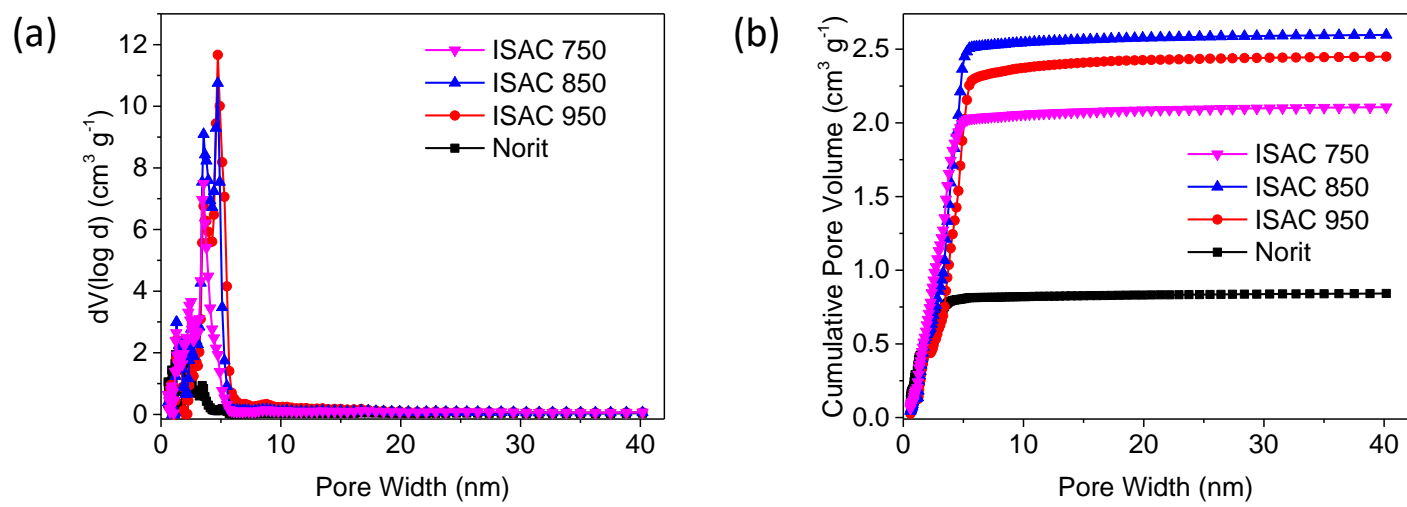


Figure S5. (a) Full-scale pore distribution and (b) cumulative pore volume profiles of ISACs

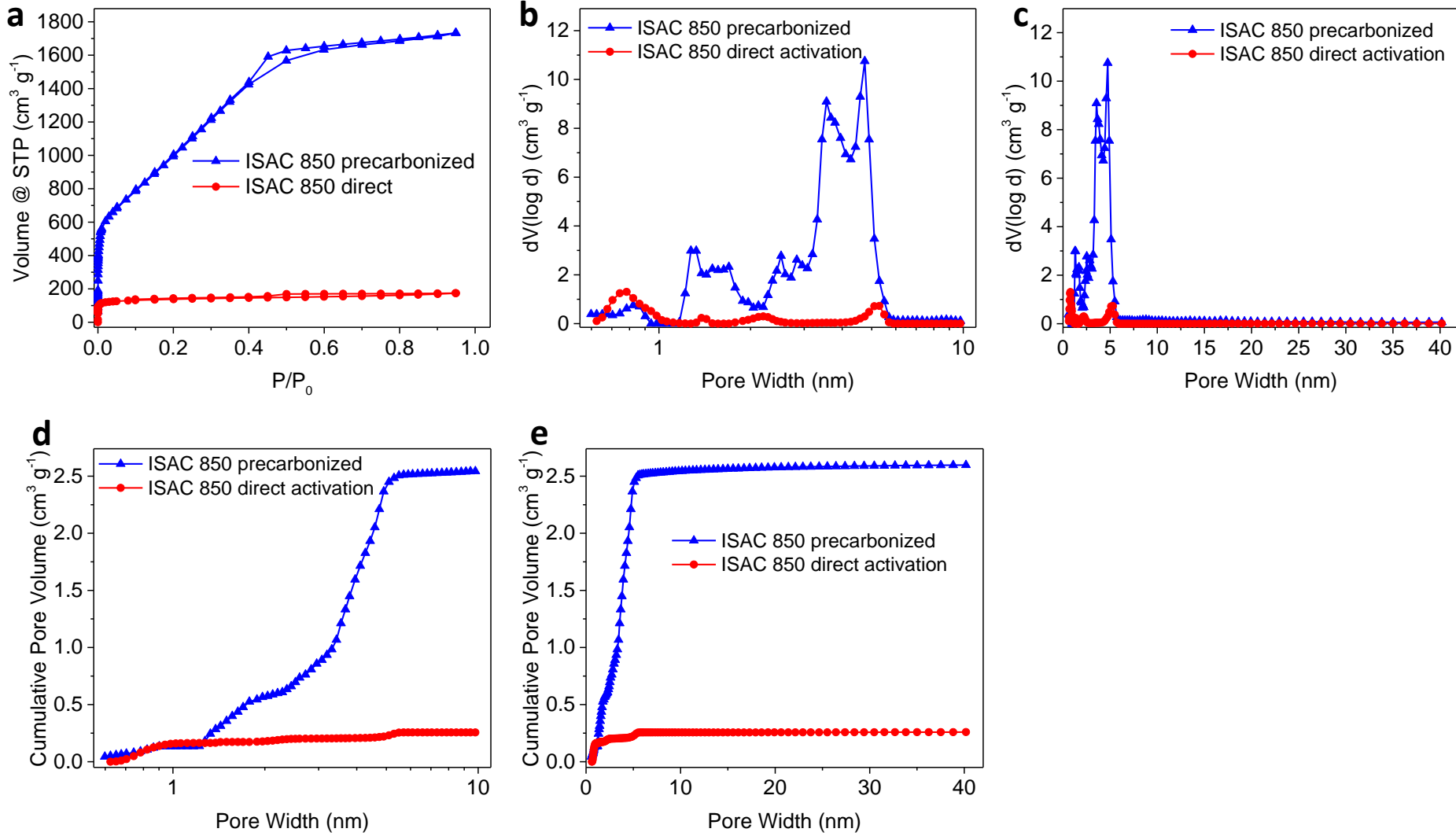


Figure S6. Comparison of ISAC 850's prepared by partial carbonization of precursor followed by separate high temperature carbonization / activation (blue) vs. simultaneous carbonization-activation of precursor (red). (a) Nitrogen adsorption-desorption isotherms, (b) expanded and (c) full scale pore size distributions, (d) expanded and (e) full scale cumulative pore volume profiles.

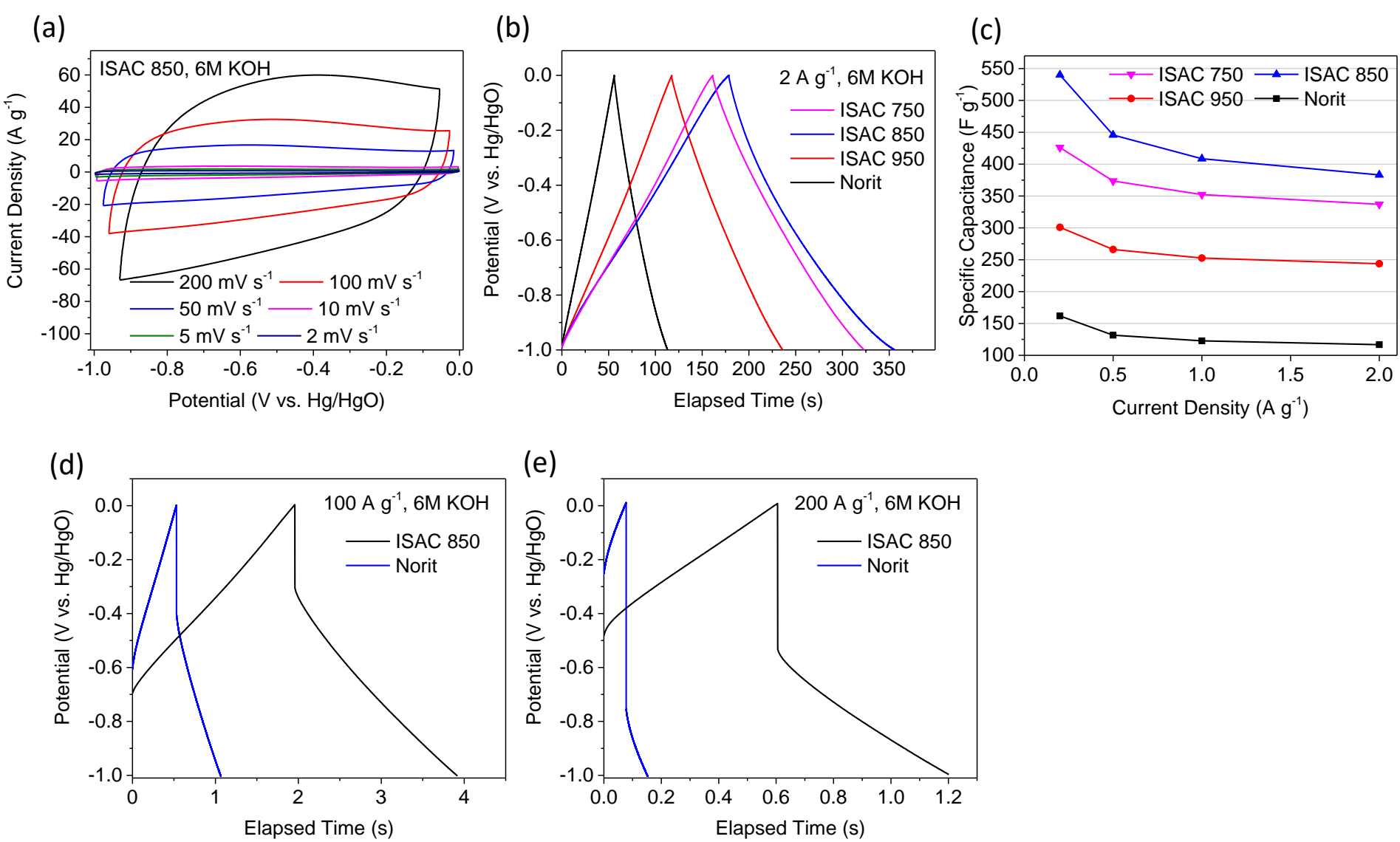


Figure S7. Electrochemical properties in a three-electrode configuration tested in 6M KOH electrolyte with a 1.0V window. (a) CVs of ISAC 850 at various scan rates. (b) Comparison of the galvanostatic curves for ISACs and Norit at 2 A g<sup>-1</sup>. (c) Low current density specific capacitances for ISACs and Norit. (d)-(e) High rate galvanostatic curves for ISAC 850 vs. Norit at current density of 100 A g<sup>-1</sup> and 200 A g<sup>-1</sup>, respectively.

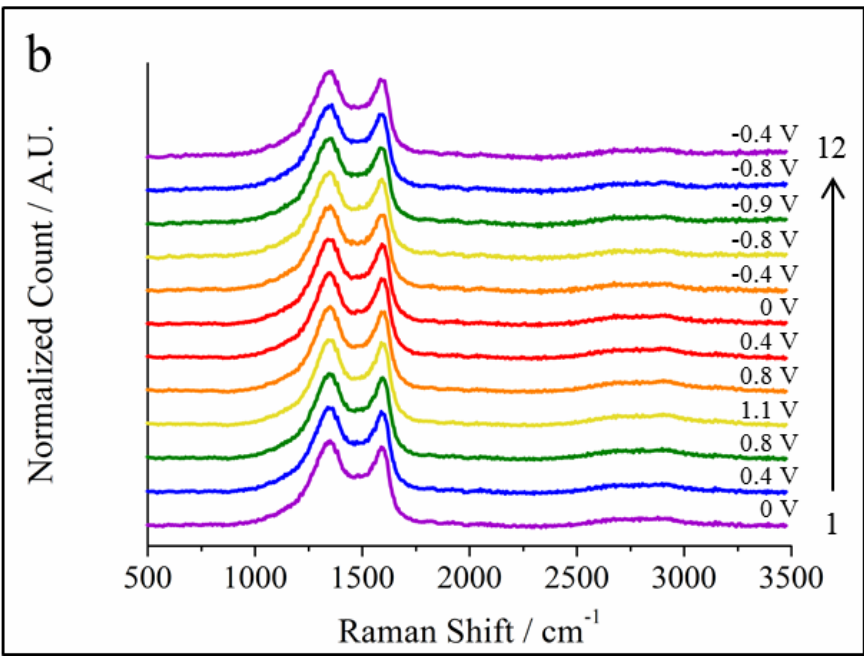
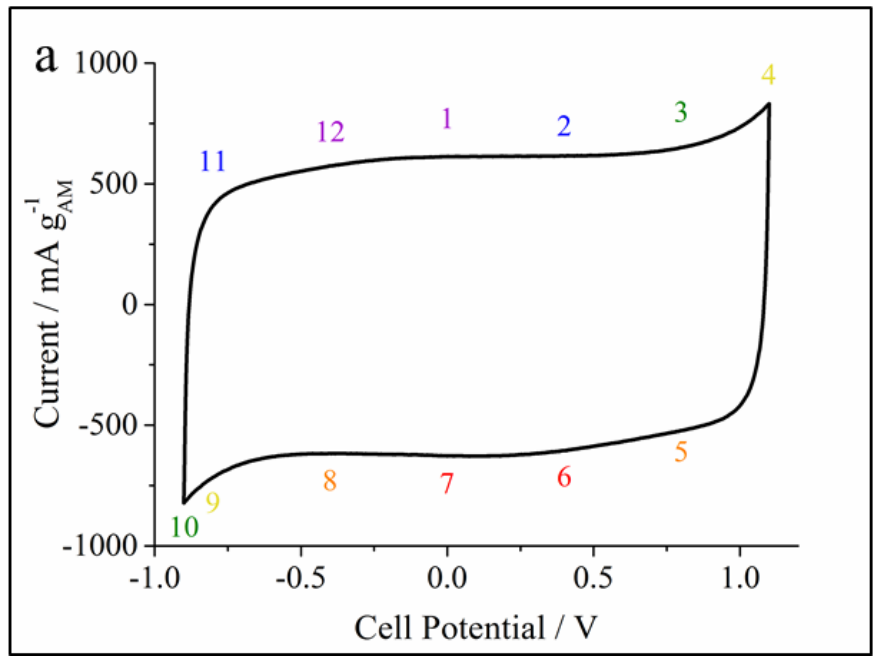


Figure S8. (a) Cyclic voltammogram collected at 20 mV/s and (b) corresponding Raman spectra acquired at potentials ranging from -0.9 – 1.1V.

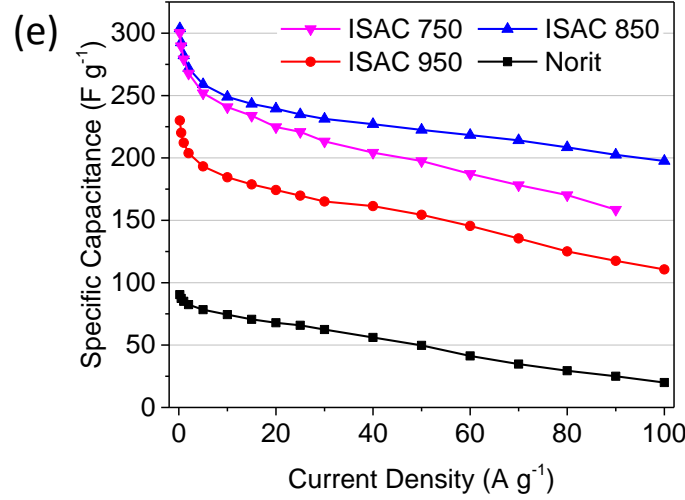
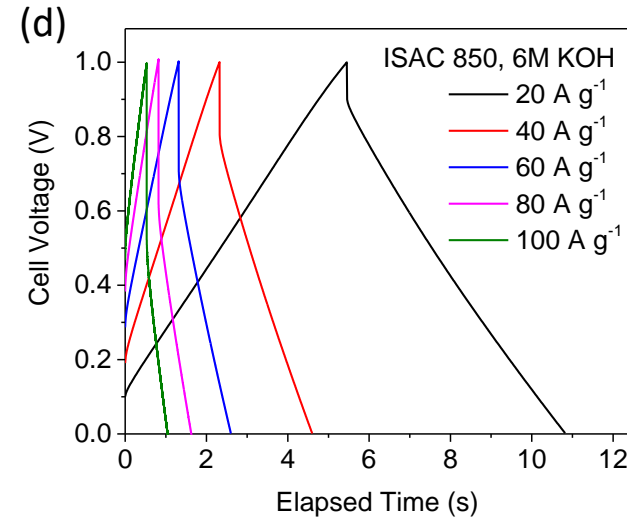
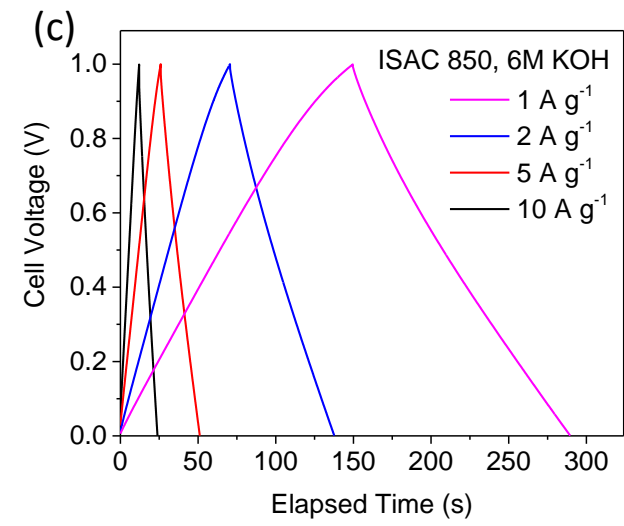
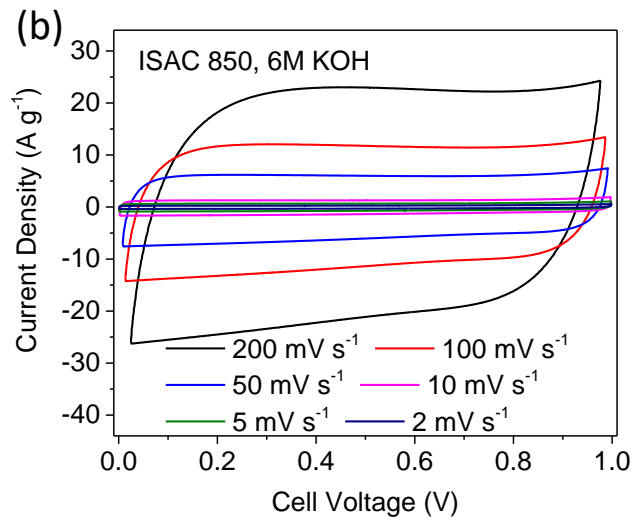
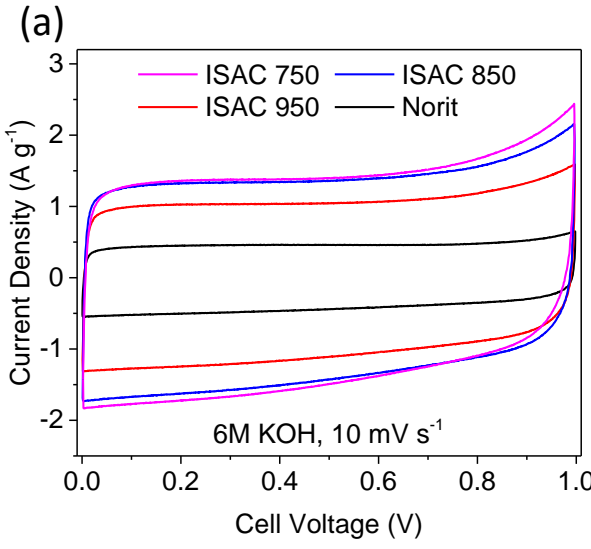


Figure S10. Electrochemical properties in symmetrical two-electrode configuration tested in 6M KOH electrolyte and 1.0V window. (a) Comparison of the CV curves for ISACs and Norit at 10 mV s<sup>-1</sup>. (b) CV profiles of ISAC 850 at various scan rates. (c) and (d) Galvanostatic data of ISAC 850 at various current densities. e) Rate capability comparison.

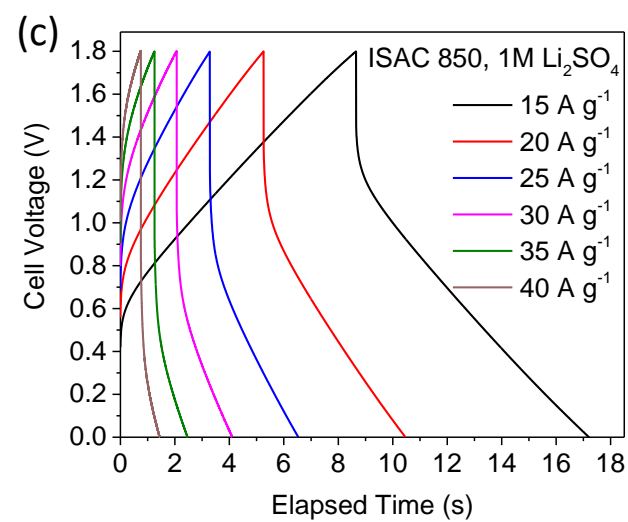
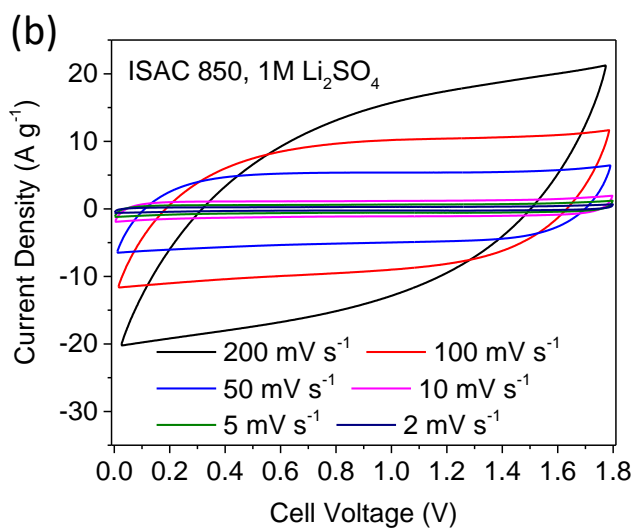
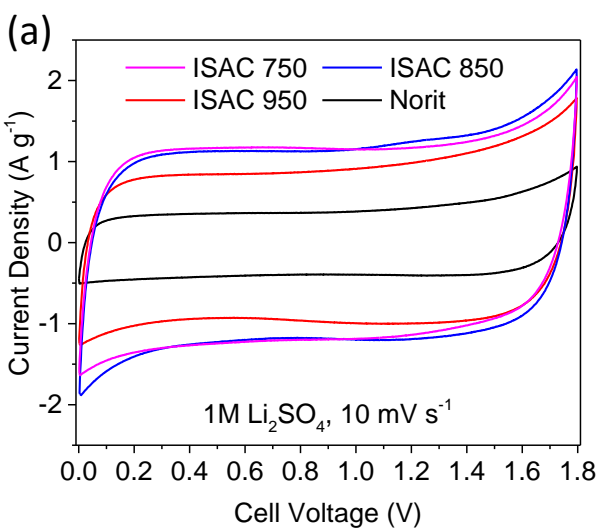


Figure S11 . (a)-(c) Electrochemical properties of ISACs in symmetrical two-electrode configuration tested in  $1\text{M Li}_2\text{SO}_4$  electrolyte with a 1.8V window. (a) CVs of ISACs and Norit at  $10 \text{ mV s}^{-1}$  scan rate. (b) CV curves of ISAC 850 at various scan rates. (c) Galvanostatic profiles of ISAC 850 at currents of  $20 - 100 \text{ A g}^{-1}$ .

<u>2-Electrode EIS in 6M KOH</u>					
Samples	$R_{ohm}^a$ ( $\Omega$ )	$R_{ct}^b$ ( $\Omega$ )	$R_{diff}^c$ ( $\Omega$ )	$ESR^d$ ( $\Omega$ )	$\nu_{onset}^e$ (Hz)
ISAC 750	0.126	0.294	0.092	0.512	3.971
ISAC 850	0.091	0.267	0.051	0.409	5.000
ISAC 950	0.117	0.362	0.080	0.558	3.971
Norit	0.123	0.342	0.292	0.757	3.154
<u>2-Electrode EIS in 1M Li<sub>2</sub>SO<sub>4</sub></u>					
Samples	$R_{ohm}^a$ ( $\Omega$ )	$R_{ct}^b$ ( $\Omega$ )	$R_{diff}^c$ ( $\Omega$ )	$ESR^d$ ( $\Omega$ )	$\nu_{onset}^e$ (Hz)
ISAC 750	0.714	2.391	0.739	3.844	0.500
ISAC 850	0.465	1.702	0.655	2.822	0.792
ISAC 950	0.623	2.547	0.751	3.921	0.792
Norit	0.425	5.475	9.618	15.518	0.199

<sup>a</sup> Ohmic resistance  
<sup>b</sup> Charge transfer resistance  
<sup>c</sup> Warburg impedance  
<sup>d</sup> Equivalent series resistance  
<sup>e</sup> Onset frequency

Table S2. Electrochemical impedance spectroscopy analysis obtained from 6M KOH and 1M Li<sub>2</sub>SO<sub>4</sub> electrolyte, symmetrical two-electrode configurations.